IMECE2002-32833

DEVELOPMENT OF LARGE-EDDY SIMULATION FOR VEHICLE AERODYNAMICS

S. Krajnović [*]
Dept. of Thermo and Fluid Dynamics
Chalmers University of Technology
SE-412 96 Göteborg
Sweden
Email: sinisa@tfd.chalmers.se

L. Davidson
Dept. of Thermo and Fluid Dynamics
Chalmers University of Technology
SE-412 96 Göteborg
Sweden
Email: lada@tfd.chalmers.se

ABSTRACT

The feasibility of use of large-eddy simulation (LES) in external vehicle aerodynamics is investigated. The computational cost needed for LES of the full size car at road conditions is beyond the capability of the computers in the near future (Krajnović (2002)). Since LES cannot be used for quantitative prediction of this flow, i.e. obtaining the aerodynamic forces and moments, an alternative use of this technique is suggested that can enhance the understanding of the flow around a car. It is found that making LES of the flow around simplified car-like shapes at lower Reynolds number can increase our knowledge of the flow around a car. Two simulations are made, one of the flow around a cube and the other of the flow around a simplified bus. The former simulation proved that LES with relatively coarse resolution and simple inlet boundary condition can provide accurate results. The latter simulation resulted in flow in agreement with experimental observations and displayed some flow features that were not observed in experiments or steady simulations of such flows. This simulation gave us possibility to study the transient mechanisms that are responsible for the aerodynamic properties of a car. The knowledge gained from this simulation can be used by the stylist to tune the aerodynamics of the car's design but also by the CFD specialists to improve the turbulence models.

INTRODUCTION

Although the Reynolds-averaged Navier-Stokes (RANS) equations used in the industrial prediction of the flow around cars, have been relatively successful, they are far from being a design tool for external aerodynamics. Flow around a car is three-dimensional with steep pressure gradients and regions of separated flows. The number of vortices are not formed only along the body and in the separation bubble in the near wake but also far from the rear face of the car. Bearman (1997) and Krajnović and Davidson (2002b) recently found large differences between time-averaged flow – containing only small number of three-dimensional vortices – and the instantaneous flow – containing large number of three-dimensional vortices at different position and size. The wide spectrum of scales in the wake region prevents construction of an accurate RANS model. All these properties together with the high levels of unsteadiness in this flow are main obstacles for accurate prediction using RANS. One illustrative example of RANS's (in)accuracy in vehicle aerodynamics is given in Han (1989) where the flow around Ahmed's body (Ahmed *et al.* (1984)) is predicted. The computed pressure at the rear vertical face of the body was (for a base slant angle smaller than 20°) under-predicted, resulting in the computed drag being 30% higher than the measured drag (Han (1989), Hucho (1998)). Thus some more accurate three-dimensional time-dependent simulation is needed.

Some early attempts to use transient simulations for this kind of flow are presented in Kataoka *et al.* (1991), Hashiguchi *et al.* (1989) and Aoki *et al.* (1993). Although the authors of these papers denoted their simulations direct numerical simulations (DNS) (Kataoka *et al.* (1991), Hashiguchi *et al.* (1989)) or large-eddy simulation (LES) (Aoki *et al.* (1993)), we would classify the simulation in Aoki *et al.* (1993) as unresolved LES and the simulations in Kataoka *et al.* (1991) and Hashiguchi *et al.* (1989) as uncontrolled LES. The simulation in Aoki *et*

---

[*] Address all correspondence to this author.

1

al. (1993) is the only simulation of this flow to our knowledge where the subgrid-scale model is employed explicitly. Transport of energy from the resolved scales to the SGS is achieved in Kataoka *et al.* (1991) and Hashiguchi *et al.* (1989) by using a third-order upwind scheme for the convection terms. The absence of a SGS model in these simulations makes it difficult to separate resolved from modeled turbulent energy.

Krajnović and Davidson (2002) estimated the computational grid needed for representation of the near wall structures in LES of the flow around cars. They shown that approximately 6×10^8 cells are needed in the near wall region of simplified car-like shape. Fortunately, they found the similarity of the flows at different Reynolds numbers. From this they concluded that LES of the flow around a car at lower Reynolds numbers can be useful for qualitative understanding of the flow around a car at high Reynolds numbers.

This paper reviews our work on the development of the LES for external vehicle aerodynamics. In the first half of the paper, we present simulations of the flow around a cube placed on the wind tunnel wall. The simulations of the flow around a cube are used to investigate the influence of the spatial resolution and the subgrid-scale model on the results. The rest of the paper presents the simulations of the flow around a simplified bus.

The present work aimed not only to investigate the feasibility of LES in vehicle aerodynamics but also to demonstrate the usefulness of LES for understanding of the flow around vehicles. Both the instantaneous and the time-averaged flows are described using our LES results, and these are compared with previous knowledge.

Finally, we end this paper with our personal opinion on the usefulness of LES in vehicle dynamics. We suggest use of LES for understanding of the flow around a car and not for obtaining quantitative information on the aerodynamic properties of the car.

FROM A CUBE TO A CAR

The choice of the test cases for the simulations was driven by the character of the flow and its similarity with the flow around a car, documentation of the flow, Reynolds number and the complexity in the geometry of the body. The shape of the body used in the simulations was chosen to be simple, allowing us to concentrate more on LES and less on the construction of the computational grid.

Flow around a cube

The first flow selected was that around the cube mounted on the wall of a wind tunnel at Reynolds number of 4×10^4 based on the incoming velocity and height of the cube. The experimental data for the time-averaged flow is reported in Larousse *et al.* (1991), Martinuzzi and Tropea (1993) and Hussein and

Martinuzzi (1996). The flow was simulated using both RANS (Hanjalić and Obi (1997)) and LES (Shah and Ferziger (1997) and Rodi *et al.* (1995)). The points of similarity between this flow and that of the flow around a car are in the separations and re-attachments and several vortices that define the dynamics of the flow, but as it is shown later in the paper, there are also many differences.

This flow was computed in Rodi *et al.* (1995) using LES resulting in a good agreement with experimental data, but as noted in Krajnović and Davidson (2002a), the extension of such LES to the higher Reynolds number flow leads to very high computational cost. Simulations in Rodi *et al.* (1995) used instantaneous results of LES of channel flow as the inlet boundary condition and very fine computation grid. Thus our study of this flow aimed to investigate if this flow can be simulated using simple inlet boundary condition and coarse computational grid.

The separation on the front edges minimize the influence of the upstream flow on the results downstream of the front face of the cube. Thus the experimental profile (constant in time) was used as inlet condition in this work. The lateral boundaries were treated as slip surfaces using the symmetry conditions $\partial \bar{u}/\partial z = \partial \bar{v}/\partial z = \bar{w} = 0$. At the downstream boundary, the convective boundary condition $\partial \bar{u}_i/\partial t + U_c (\partial \bar{u}_i/\partial x) = 0$ was used. Here, U_c was set equal to the mean bulk velocity, U_b. No-slip conditions were used at the solid walls. The homogeneous Neumann condition was used for the pressure at all boundaries. The extent of the computational domain was, similar to the simulations in Rodi *et al.* (1995), three cube heights upstream of the cube, six cube heights downstream and seven cube heights laterally (see Fig. 1). The grid used in the simulations was four times smaller (0.27×10^6 cells) than the grids from Rodi *et al.* (1995). The distance of the nearest grid point from the solid wall was $0.023H$ which is approximately two times the distance in simulations in Rodi *et al.* (1995) (see Rodi (1997)). The inadequate resolution is compensated for by the use of a dynamic one-equation SGS model. Two one-equation subgrid models, described in Davidson (1997) and Menon and Kim (1996), are used to model the subgrid-scale stress tensor. Both models are subgrid-scale kinetic energy models. The SGS stress tensor is modeled as $\tau_{ij} = -2\nu_{sgs}\bar{S}_{ij}$ with the eddy viscosity defined as $\nu_{sgs} = C\Delta k_{sgs}^{\frac{1}{2}}$ and SGS kinetic energy as $k_{sgs} = 1/2\tau_{ii}$. A detailed description of these models can be found in Krajnović and Davidson (2002a).

Figure 2 compares the time-averaged streamlines in the symmetry plane for two LES and experiments. Both simulations predicted the horseshoe vortex and the separation regions on the roof, lateral sides and behind the cube in agreement with the experiments (Fig. 2). The predicted separation lengths X_{F1} and X_{R1} (Figs. 2c) differed $6-7\%$ and $14-16\%$, respectively, between our LES and experiments. The same lengths were in Rodi *et al.* (1995) predicted within $1-29\%$ accuracy for X_{F1} and $7-13\%$

accuracy for X_{R1}. The main difference in the picture of the time-averaged flow between experiment and LES is in the size of the horseshoe vortex. The separation between the two legs of this vortex at $0.75H$ downstream of the cube is 36% larger in the predicted flow than in the experiment. This difference at $4.3H$ downstream of the cube is decreased to only 2%. The difference in the location of the horseshoe legs was explained by findings of Martinuzzi and Tropea (Martinuzzi and Tropea (1993)) who found that the shape of the horseshoe vortex is strongly influenced by the oncoming boundary layer.

Figure 1. Geometry of a cube placed on a wind tunnel wall. Predicted time-averaged trace lines are plotted on the surface of the body showing the roof and the lateral vortices. View of the front face of the cube.

Comparison of the coherent structures of the time-averaged flow in experiments and LES is presented in Fig. 3. The horseshoe vortex H, two lateral side vortices L, the roof vortex T and the arch vortex W in the separation bubble behind the body are all accurate predicted in LES. The cores of these vortices are visualized in this figure using the critical point theory (Chong *et al.* (1990), Sujudi and Haimes (1995)), i.e. we plotted the points whose rate-of-deformation tensor has one real and a pair of complex-conjugate eigenvalues and whose velocity is zero.

The instantaneous flow (Fig 4) differs from the time-averaged one. The time-averaged vortices L and T (Fig. 3) are averaged from a number of instantaneous vortices L_i and T_i, respectively, in Fig. 4. The flow separates on the sharp front edges and form the instantaneous vortices T_i and L_i. As they are transported downstream, these vortices break down and interact with each other. They produce fluctuating forces on the body. The
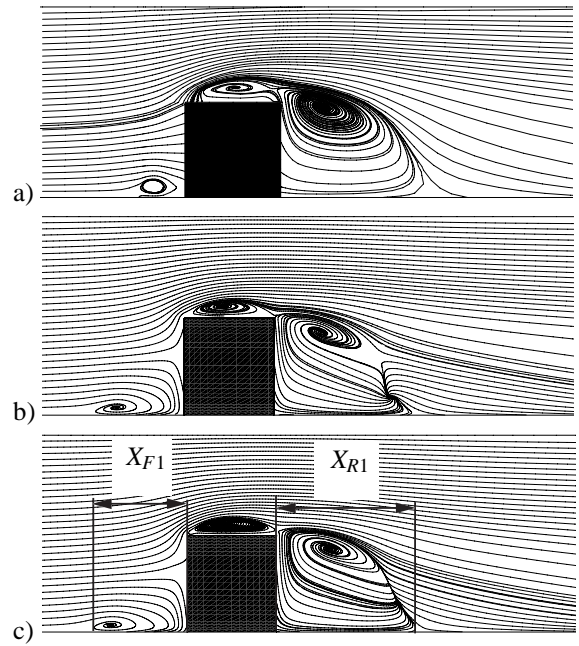

Figure 2. Streamlines of the mean flow projected onto the center plane of the cube using: a) experiment of Hussein and Martinuzzi (1996); b) model from Menon and Kim (1996); c) model from Davidson (1997) (Note that the streamlines in Figs. b and c are emitted from the same positions in the flow.).

side force signal was Fourier transformed, and a peak is found in the spectrum. The Strouhal number of this periodic component was found to be 0.134 as compared to the experimental value of 0.145. For comparison we can mention that no shedding frequency was reported in previous LES (Shah and Ferziger (1997)) while the shedding period corresponding to a Strouhal number of 0.17 was observed in the unsteady RANS simulation in Iaccarino and Durbin (2000).

The present simulations showed that LES using simple inlet boundary conditions, a relatively coarse grid and one-equation SGS model gives accurate results. Although these results are encouraging, the conclusions of the feasibility of the LES of the flow around a car cannot be drawn from these results, owing to the difference in the flow and the geometry between the two flows. The car-body is lifted from the floor and the flow coming from under the body makes the instantaneous wake longer than in the flow behind the cube. The position of the car-body makes the wake more instantaneous with one additional degree of freedom (in the negative y direction). The absence of the sharp edges, such as those on a cube, on a car-body can result in smaller regions of separated flow close to the front face of a car. Thus the influence of the upstream flow and thereby inlet boundary condition on the wake flow can be larger. Besides the physics of the flow which is changed with the geometry of the body, the cho-
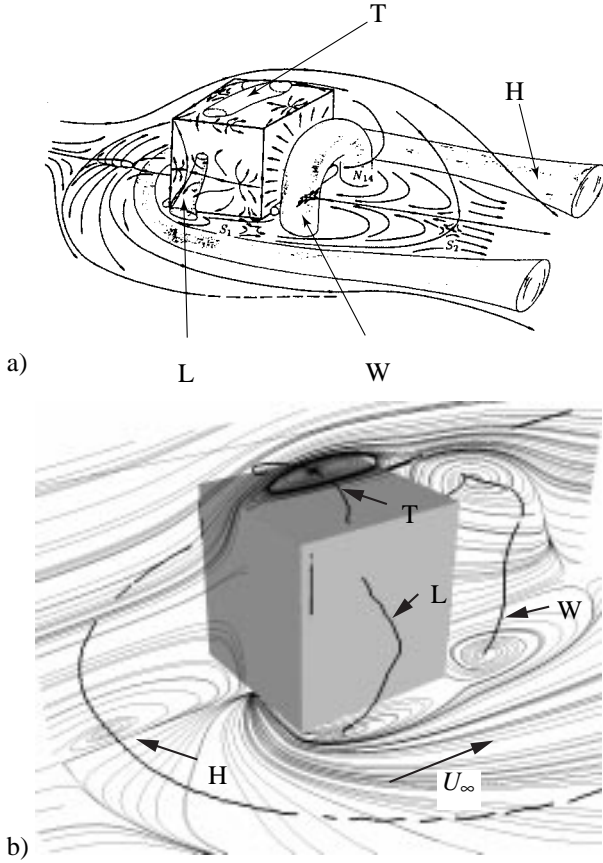
a)

b)

Figure 3. a) Schematic representation of the flow features by Martinuzzi and Tropea (from Hussein and Martinuzzi (1996) with permission by Physics of Fluids). View of the rear face of the body. b) Predicted time-averaged streamlines projected onto planes $x = 0$ and $z = 0$. The black curves represent the vortex cores. View of the front face of the body.

Figure 4. Predicted instantaneous second invariant of the velocity gradient $Q = 5$. View of the front face of the body.

ice of the numerical method is also influenced. The shape of the cube made it possible for us to use a single-block Cartesian code that was optimized for this kind of flow. The computation of the flow around a complex geometry car at higher Reynolds number (thus more cells) calls for use of a code that is parallelized using block decomposition and PVM or MPI message passing systems such as that used in our next test case.

Flow around a simplified bus

A flow around a bus-shaped body (Duell (1994), Duell and George (1999)) was chosen as a second test case. This flow is similar to the flow around a real vehicle and there is some knowledge of this kind of flow from previous experimental and numerical studies (Bearman *et al.* (1983), Ahmed *et al.* (1984), Barlow *et al.* (1999), Duell *et al.* (1999, 1989)). As the flow is characterized by a fairly high Reynolds number (0.21×10^6, based on the model height H and the incoming velocity), the re-
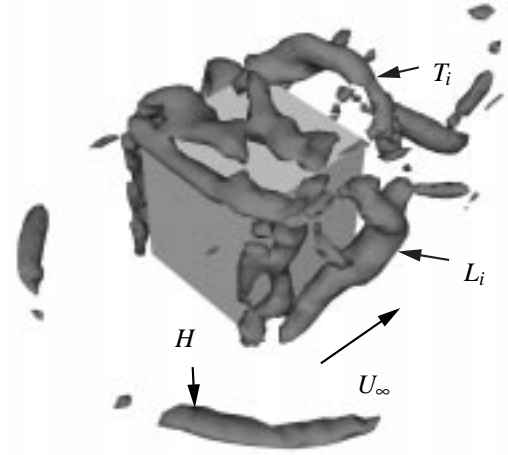
sulting flow features and the character of the flow-induced forces on the body should be similar as in the flow around a full-scale vehicle.

The shape of the body is based on the Ahmed's body (Ahmed *et al.* (1984)) and it is shown placed above the wind tunnel wall in Fig. 5. A computational domain with an upstream length of $8H$, a downstream length of $21H$ and a spanwise width of $5.92H$ was used for the simulations. A moving ground belt in the experiment (Duell (1994), Duell and George (1999)) was simulated in the simulations by applying the inlet velocity U_∞ on the floor. The near-wall spatial resolution expressed in the wall units was $\langle \Delta s^+ \rangle_t = 5 - 164$ in the streamwise direction, $\langle \Delta n^+ \rangle_t = 0.5 - 0.8$ in the wall-normal direction and $\langle \Delta l^+ \rangle_t = 14 - 142$ in the spanwise direction. Here $\Delta f^+ = \Delta f u_\tau / \nu$, u_τ is the friction velocity and $\langle . \rangle_t$ denotes time averaging. The no-slip boundary conditions were applied on the solid walls. The Smagorinsky model (Smagorinsky (1963)) for the SGS stress tensor was chosen for its simplicity and low computational cost.

The flow separates at the rounded side and roof edges of the body and forms transversal vortices (Fig. 6a) similar to Kelvin-Helmholtz vortices found on the Ahmed's body in Spohn and Gillieron (2002). These vortices are lifted further back, forming hairpin vortices in Fig. 6b. They average to three separation regions shown in Fig. 7. Two kinds of critical points (Perry and Chong (1987)) are visible in this figure. These are one unstable node Z at the upper-side edge of the bus and saddle points S_d and S_s downstream of the separation regions R and L, respectively.

Two counter-rotating longitudinal vortices (Fig. 8a) are formed along the upper-side edges and one longitudinal vortex (Fig. 8b) along the lower edge, on each side of the bus. The existence of similar longitudinal vortices on the roof of the body was observed in the experiment of the Ahmed's body flow (Spohn and Gillieron (2002)) while the lower-edge longi-
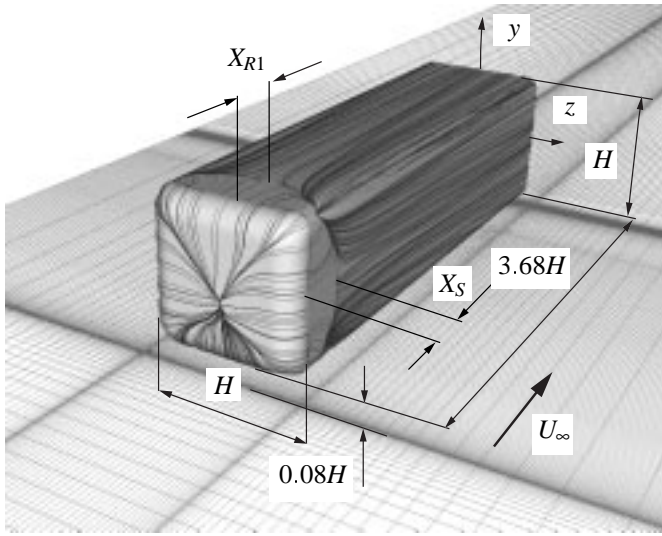
4

Figure 5. Geometry of the bus-shaped body placed above the wind tunnel wall. Predicted time-averaged trace lines are plotted on the surface of the body showing the roof and the lateral vortices that extend X_{R1} and X_S, respectively in the streamwise direction.

tudinal vortices were registered in previous numerical study of Han (1989).

The instantaneous near wake region was found to consist of large scale coherent structures with their axes parallel with the separation edges on the rear face of the body. These structures average to the vortex ring (Krajnović and Davidson (2002c), Krajnović and Davidson (2002b)) in agreement with the experimental observations (Duell (1994), Duell and George (1999), Ahmed *et al.* (1984)). Besides this large vortex, four thin vortices (*B* in Fig. 9) were observed close to the rear edges. Note that only two of these vortices (vortices with cores parallel with *z* axes) are shown in this figure. Our simulation showed that these vortices are very unsteady and thus cannot be captured in RANS simulations. They are not observed in the experiment (Duell (1994), Duell and George (1999)) probably because of the measurement technique used (hot-wire anemometry) and the fact that they are very close to the wall. The streamwise length of the separation bubble in Fig. 9, X_r was overpredicted by some 7% compared to experiment (Duell (1994), Duell and George (1999)). This was explained in Krajnović and Davidson (2002b) by somewhat coarse computational grid in the spanwise direction and experimental uncertainty.

After the closure of the bubble, a pair of the counter-rotating longitudinal vortices was observed in the time-averaged flow in agreement with the experimental observations of the similar flows (Ahmed (1981), Ahmed *et al.* (1984), Barlow *et al.* (1999), Bearman (1997)). The observation of Bearman (1997) that the instantaneous vortices are very different from the coherent structures that appear in the instantaneous flow, was confir-
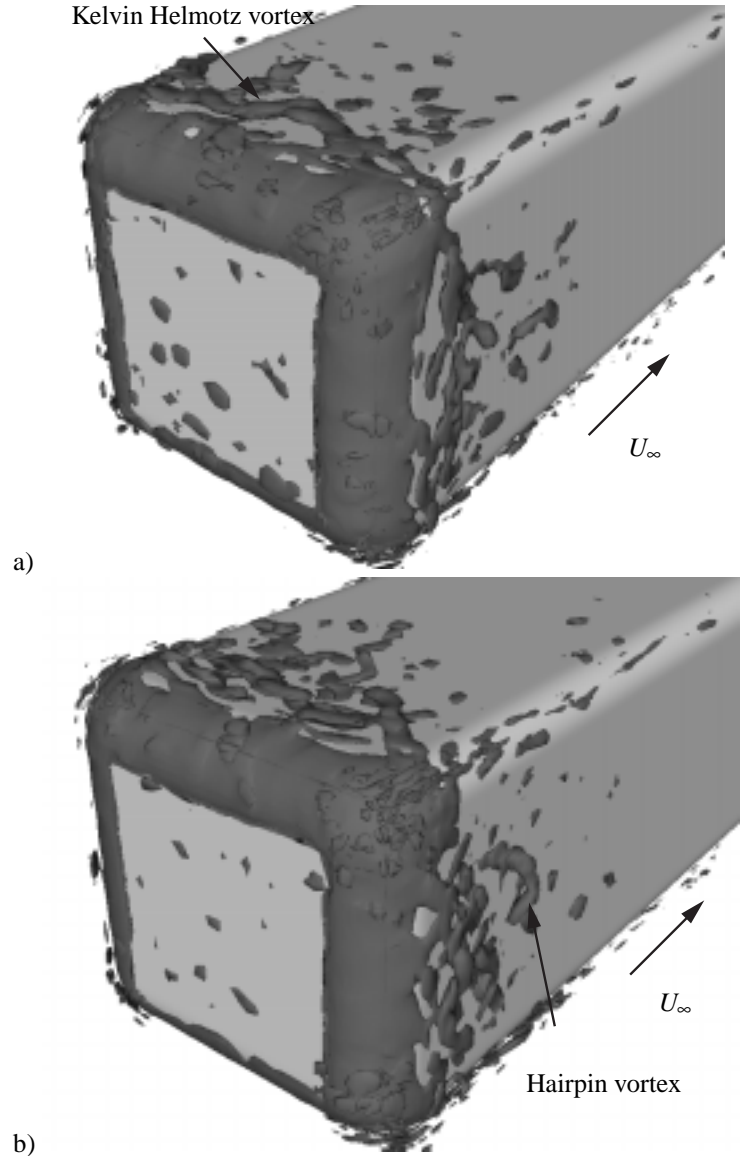

a)

b)

Figure 6. Predicted instantaneous vortices formed after the separation on the front edges of the body. Isosurface of second invariant of the velocity gradient $Q = 8000$. The time-difference between two pictures is $tU_\infty/H = 0.8$

med in this simulation (see Krajnović and Davidson (2002b)). For additional details on the flow features and the mechanisms of their origin, we refer to Krajnović and Davidson (2002b) and here it should suffice to say that the LES gave accurate representation of the coherent structures in this flow and explained their formation and interaction.

Now, we shall consider the ability of LES to predict the aerodynamic forces and their variation. In absence of experimental data from experiments in Duell (1994) and Duell and George
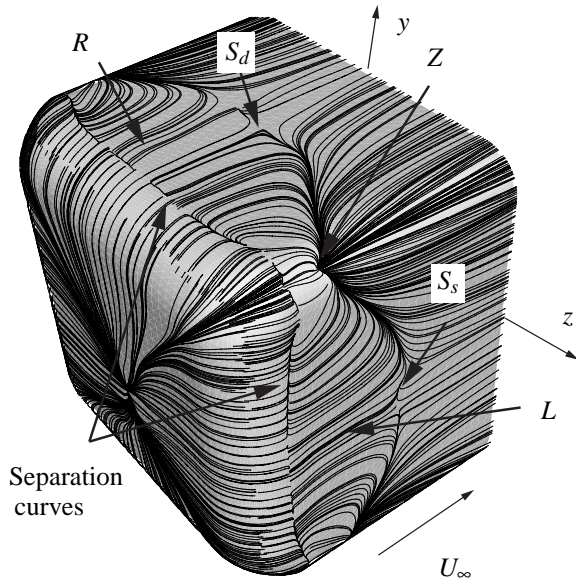
5

Figure 7. Predicted time-averaged trace lines on the surface of the body showing the roof vortex, R and the lateral vortex, L. View of the front face of the body.

Figure 8. Predicted time-averaged streamlines projected onto planes. a) $x = -1.28H$. The rotation of U_p and U_s is counter-clockwise and clockwise, respectively. View from behind of the upper-right edge of the body. b) $x = -0.48H$. The direction of the rotation of this vortex is counter-clockwise. View from behind of the lower-right edge of the body.

(1999), the time-averaged drag and lift coefficients were compared with those in experiments of Barlow *et al.* (1999) for a similar body. The drag coefficient was found to be identical with the one in Barlow *et al.* (1999) whereas the lift coefficient was some 8% underpredicted. Note that the floor in the experiment of Barlow *et al.* (1999) was stationary unlike the moving floor in the experiment of Duell and George (1999) and it is known (see Bearman *et al.* (1989)) that the moving floor influences the flow (For example Bearman *et al.* (1989) found that floor movement reduces drag by 8% and lift by 30% in a case of 1/3rd scale car model). The signals of the forces acting on the bus was Fourier transformed, and two main frequencies at Strouhal numbers 0.22 and 0.6 were observed in the side-force signal, of which 0.22, is close to the shedding frequency of 0.23 found in Bearman's experimental study of the wake behind a car model (Bearman (1997)). The value of the pressure coefficient integrated over the rear face of the bus for which experimental data exist from Duell (1994) and Duell and George (1999), was overpredicted in our LES by 5% of the dynamic pressure. This can be explained with the boundary layers that exist in the experiment on the side walls of the wind tunnel, which in the simulations were not resolved but replaced with slip conditions. More results on the transient forces, velocities and stresses can be found in Krajnović and Davidson (2002b).
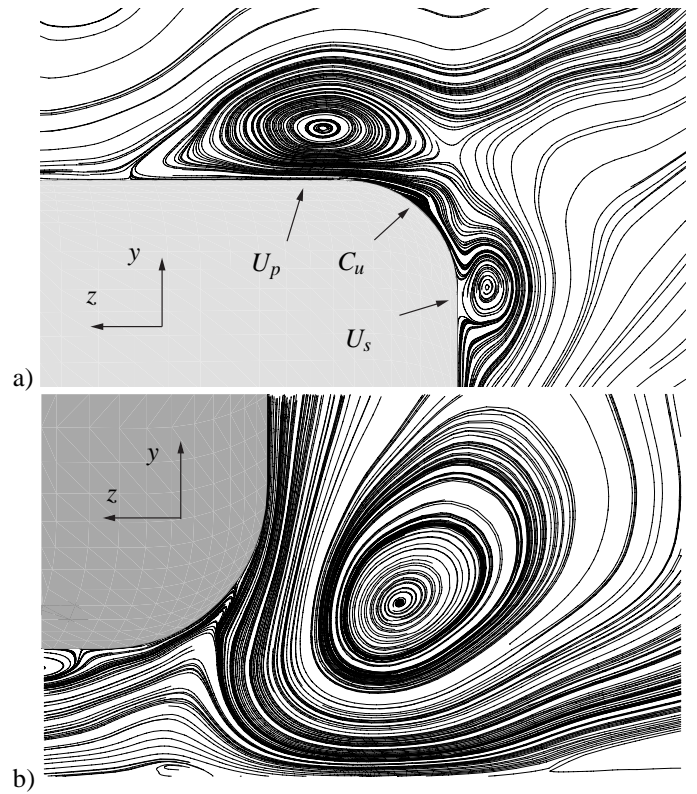
PERSPECTIVES ON LES FOR VEHICLE AERODYNAMICS

The conclusion from this paper is that the near future of LES in vehicle aerodynamics is in the exploration of the physics of such flow. Making LES of the flow around vehicle models at lower Reynolds number, such as the simulation presented in this paper, is likely to be most useful. The strength of LES is that the transient processes can be studied in detail which is difficult in experiments and impossible in RANS. Similar to DNS used for accumulation of fundamental knowledge on turbulence physics, LES will be used for obtaining the fundamental knowledge on car's flow physics. The idea is to use the gained understanding of the flow at lower (LES feasible) Reynolds number for modeling of the flow at high Reynolds number and for helping the stylist to improve the aerodynamic properties when designing the car.

Although the commercial codes have began to include LES models, the use of LES in external vehicle aerodynamics of full size vehicles will be limited to qualitative understanding of the flow around small parts of vehicle such as mirrors. The automotive industry will continue (at least in next decade) to rely on
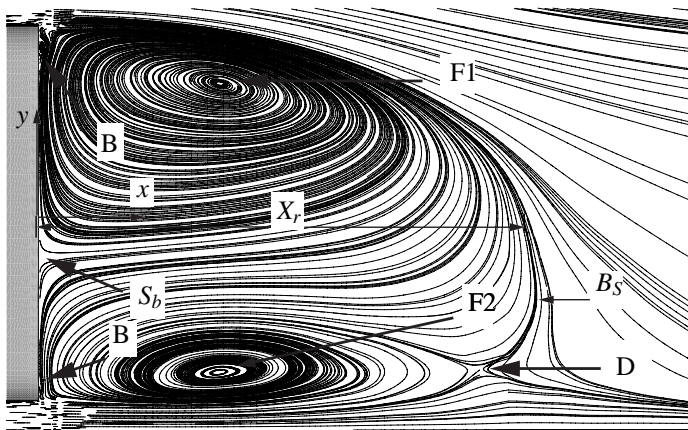
6

Figure 9. Predicted time-averaged streamlines projected onto symmetry plane $z = 0$ of the bus. S_b is the stagnation point on the rear face of the bus, B_S is the free stagnation point, D is the saddle point and F1 and F2 are foci of the upper and lower vortices, respectively.

the experimental studies for the quantitative aerodynamic data such as drag and lift coefficients. Computational fluid dynamics (CFD) will not be used to predict the forces and moments acting on a car but to explain the reasons for these and to lay down the outlines for their controlled change (by the stylist).

As the computer power increases the higher Reynolds number (Re) flow around a car can be simulated using LES, but reaching the Reynolds number of the flow around a passenger car (approximately $Re = 5 \times 10^6$, see Krajnović (2002)) requires an alternative simulation technique for the near-wall region, that necessarily include certain amount of empiricism. Several hybrid methods entitled hybrid LES/RANS (Davidson and Peng (2001)) methods or detached-eddy simulation (DES) (Spalart *et al.* (1997)) are suggested, where the boundary layer (or a part of it) is modeled using RANS (in transient mode) and the separated flow away from the wall is simulated with LES. Many unresolved issues such as the optimal position of the matching line between LES and RANS in hybrid LES/RANS, the choice of the RANS turbulence model or construction of the suitable computational grid, remain to be solved before these hybrid methods can be used for complex flow simulations.

Until an efficient and accurate way of modeling of near-wall mechanisms is found, LES will be used in vehicle aerodynamics as a powerful complement to the experiments that enable us to understand this complex flow.

ACKNOWLEDGMENTS

REFERENCES

Ahmed, S. (1981). Wake structures of typical automobile shapes. *ASME: Journal of Fluids Engineering 103*, 162–169.

Ahmed, S. R., G. Ramm, and G. Faltin (1984). Some salient features of the time averaged ground vehicle wake. SAE Paper 840300.

Aoki, K., T. Ohbayashi, M. Zhu, and H. Miyata (1993). Finite-volume simulation of 3-d vortical flow-fields about road vehicles with various after-body configuration. SAE Paper 931896.

Barlow, J., R. Guterres, R. Ranzenbach, and J. Williams (1999). Wake structures of rectangular bodies with radiused edges near a plane surface. SAE Paper 1999-01-0648.

Barlow, J. B., R. Guterres, and R. Ranzenbach (1999). Rectangular bodies with radiused edges in ground effect. AIAA paper 99-3153.

Bearman, P. W. (1997). Near wake flows behind two- and three-dimensional bluff bodies. *Journal of Wind Engineering and Industrial Aerodynamics 69-71*, 33–54.

Bearman, P. W., D. D. Beer, E. Hamidy, and J. K. Harvey (1989). The effect of a moving floor on wind-tunnel simulation of road vehicles. SAE Paper No. 880245.

Bearman, P. W., J. P. Davis, and J. K. Harvey (1983). Measurement of the structure of road vehicle wakes. *International Journal of Vehicle Design,Technological Advances in Vehicle Design Series, SP3, Impact of Aerodynamics on Vehicle Design*, 493–499.

Chong, M. S., A. E. Perry, and B. J. Cantwell (1990). A general classification of three-dimensional flow fields. *Physics of Fluids 5*(2), 765–777.

Davidson, L. (1997). Large eddy simulation: A dynamic one-equation subgrid model for three-dimensional recirculating flow. In *11th Int. Symp. on Turbulent Shear Flow*, Volume 3, Grenoble, pp. 26.1–26.6.

Davidson, L. and S.-H. Peng (2001). A hybrid LES–RANS model based on a one-equation SGS model and a two-equation $k - \omega$ model. In E. Lindborg, A. Johansson, J. Eaton, J. Humphrey, N. Kasagi, M. Leschziner, and M. Sommerfeld (Eds.), *The Second International Symp. on Turbulence and Shear Flow Phenomena*, Volume 2, Stockholm, pp. 175–180.

Duell, E. G. (1994). *Experimental investigation of unsteady near wakes of ground vehicle bodies*. Ph. D. thesis, Cornell University.

Duell, E. G. and A. R. George (1999). Experimental study of a ground vehicle body unsteady near wake. SAE Paper 1999-01-0812.

Han, T. (1989). Computational analysis of three-dimensional turbulent flow around a bluff body in ground proximity.

7

AIAA Journal 27(9), 1213–1219.

Hanjalić, K. and S. Obi (1997). ERCOFTAC/IAHR/COST workshop on refined flow modeling. Delft University of Technology, pp. 131–225.

Hashiguchi, M., K. Kawaguchi, R. Yamasake, and K. Kuwahara (1989). Computational study of the wake structure of a simplified ground-vehicle shape with base slant. SAE Paper 890597.

Hucho, W.-H. (1998). *Aerodynamics of Road Vehicles* (4 ed.). Society of Automotive Engineers, Inc. ISBN 0-7680-0029-7.

Hussein, H. and R. J. Martinuzzi (1996). Energy balance for turbulent flow around a surface mounted cube placed in a channel. *Physics of Fluids 8*(3), 764–780.

Iaccarino, G. and P. Durbin (2000). Unsteady 3D RANS simulations using the $v^2 - f$ model. In *Annual Research Briefs 2000*, Stanford University, pp. 263–269.

Kataoka, T., H. China, K. Nakagawa, K. Yanagimoto, and M. Yoshida (1991). Numerical simulation of road vehicle aerodynamics and effect of aerodynamic devices. SAE Paper 910597.

Krajnović, S. (2002). *Large Eddy Simulations for Computing the Flow Around Vehicles*. Ph. D. thesis, Dept. of Thermo and Fluid Dynamics, Chalmers University of Technology, Gothenburg.

Krajnović, S. and L. Davidson (2002a). Large eddy simulation of the flow around a bluff body. *AIAA Journal 40*(5), 927–936.

Krajnović, S. and L. Davidson (2002b). Numerical study of the flow around the bus-shaped body. submitted for journal publication.

Krajnović, S. and L. Davidson (2002c). A test case for large-eddy simulation in vehicle aerodynamics. In *Proceedings of the 5th International Symposium on Engineering Turbulence Modelling and Measurements*, Mallorca, Spain.

Larousse, A., R. Martinuzzi, and C. Tropea (1991). Flow around surface-mounted, three-dimensional obstacles. In *9th Int. Symp. on Turbulent Shear Flow*, Munich, pp. 127–139. Springer-Verlag.

Martinuzzi, R. and C. Tropea (1993). The flow around surface-mounted prismatic obstacles placed in a fully developed channel flow. *ASME: Journal of Fluids Engineering 115*(1), 85–91.

Menon, S. and W.-W. Kim (1996). High Reynolds number flow simulations using the localized dynamic subgrid-scale model. 34th Aerospace Sciences Meeting, AIAA Paper 96-0425, Reno.

Perry, A. E. and M. S. Chong (1987). A description of eddying motions and flow patterns using critical-point concepts. *Ann. Rev. Fluid Mech. 19*, 125–155.

Rodi, W. (1997). Large-eddy simulations of the flow past bluff bodies: State-of-the-art. In *Proc. JSME Centennial Grand Conf., Int. Conf. Fluid Eng.*, Tokyo.

Rodi, W., J. H. Ferziger, M. Breuer, and M. Pourquié (1995). Workshop on LES of flows past bluff bodies. Rotach-Egern, Germany.

Shah, K. B. and J. H. Ferziger (1997, April). A fluid mechanicians view of wind engineering: Large eddy simulation of flow past a cubic obstacle. *Journal of Wind Engineering and Industrial Aerodynamics 67*, 211–224.

Smagorinsky, J. (1963). General circulation experiments with the primitive equations. *Monthly Weather Review 91*(3), 99–165.

Spalart, P. R., W. H. Jou, M. Strelets, and S. R. Allmaras (1997). Detached-eddy simulation of an airfoil at high angle of attack. In *Advances in DNS/LES, Proceedings of the First AFOSR International Conference on DNS/LES*.

Spohn, A. and P. Gillieron (2002). Flow separations generated by a simplified geometry of an automotive vehicle. In *IUTAM Symposium: Unsteady Separated Flows*, April 8-12, Toulouse, France.

Sujudi, D. and R. Haimes (1995). Identification of swirling flow in 3-D vector fields. AIAA Paper AIAA 95-1715.